Appl. Numer. Math. 203 (2024) 69–83

Contents lists available at ScienceDirect

Applied Numerical Mathematics

journal homepage: www.elsevier.com/locate/apnum

Research Paper

Approximation of piecewise smooth functions by nonlinear bivariate C^2 quartic spline quasi-interpolants on criss-cross triangulations

Francesc Aràndiga [a], Sara Remogna [b,*]

[a] *Departament de Matemàtiques, Universitat de València (EG), Spain*
[b] *Dipartimento di Matematica "G. Peano", Università degli Studi di Torino, Italy*

A R T I C L E I N F O

Keywords:
Spline quasi-interpolation
WENO
Piecewise smooth functions approximation

A B S T R A C T

In this paper we focus on the space of C^2 quartic splines on uniform criss-cross triangulations and we propose a method based on weighted essentially non-oscillatory techniques and obtained by modifying classical spline quasi-interpolants in order to approximate piecewise smooth functions avoiding Gibbs phenomenon near discontinuities and, at the same time, maintaining the high-order accuracy in smooth regions. We analyse the convergence properties of the proposed quasi-interpolants and we provide some numerical and graphical tests confirming the theoretical results.

1. Introduction

In many mathematical and scientific applications, the accurate approximation of bivariate data and functions is required. In this context, interpolation and quasi-interpolation are powerful techniques, well known and studied in the literature. In particular, if we compare them, quasi-interpolation (see e.g. the recent book [11]) does not require the solution of any system of equations and does not require that the approximant exactly matches the data at certain points. These properties are attractive in the multivariate case where the number of data can be huge and if we deal with noisy data.

In this paper we focus on the space of C^2 quartic splines on uniform criss-cross triangulations of a rectangular domain (see e.g. [1,6,7,15,20,21,23,25,26] and references therein) and we propose a method obtained by modifying classical spline quasi-interpolants (QIs) in order to approximate piecewise smooth functions avoiding Gibbs phenomenon near discontinuities and, at the same time, maintaining the high-order accuracy in smooth regions. Such a method is based on Weighted Essentially Non-Oscillatory (WENO) techniques in the definition of the spline QI. We remark that the peculiar characteristic of the proposed method is the possibility of dealing with discontinuities without knowing where they are. Indeed, the smoothness indicators are able to detect the region of discontinuity and the coefficient functionals (defining the spline QI) are automatically modified by the WENO technique. In this way, thanks to the general expression of the nonlinear coefficient functionals, the spline quasi-interpolant is automatically constructed, with its coefficient functionals adjusted according to the possible discontinuity.

The proposed technique has been proposed in [4] in the univariate setting, considering C^1 quadratic and C^2 cubic spline quasi-interpolants. Then, in [5] the problem has been faced in the bivariate case, considering the space of C^1 quadratic splines on criss-cross triangulations and now we propose the application of such a technique in a spline space allowing higher smoothness C^2.

* Corresponding author.
E-mail addresses: arandiga@uv.es (F. Aràndiga), sara.remogna@unito.it (S. Remogna).

https://doi.org/10.1016/j.apnum.2024.05.018
Received 15 January 2024; Received in revised form 20 May 2024; Accepted 20 May 2024

Available online 24 May 2024

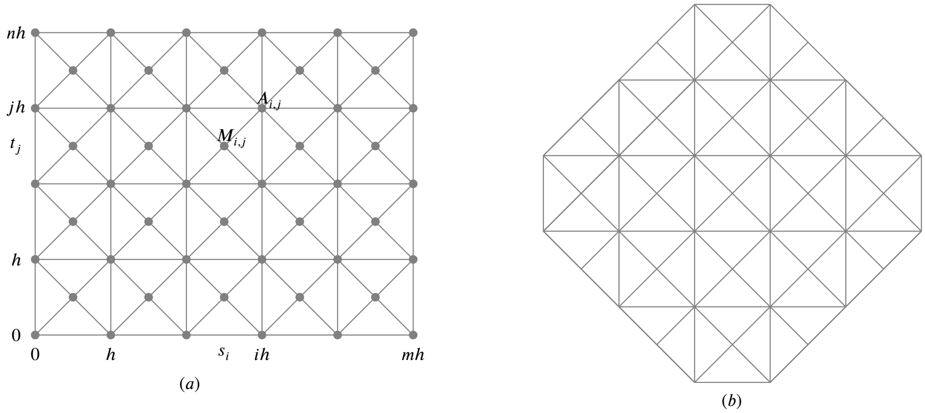

Fig. 1. (*a*) Uniform criss-cross triangulation and data points; (*b*) support of the C^2 quartic box spline B_1.

Moreover, we can cite other papers in the literature collocated in this field using quasi-interpolation but based on radial basis functions (RBFs). For example, in [14], the authors propose a shape preserving quasi-interpolation operator based on a new transcendental RBF and the numerical experiments reveal that it not only gives very accurate results but also it does not suffer of the Runge and Gibbs phenomena (see also [8,18,27]).

The paper is organized as follows. In Section 2 we define the spline space and recall definition and properties of spline quasi-interpolating operators. Then, in Section 3 we apply WENO techniques for constructing nonlinear spline quasi-interpolants and we study their properties. In Section 4 we give some numerical and graphical tests confirming the theoretical results of Section 3. Finally, in Section 5 we present some conclusions.

2. The spline space and linear quasi-interpolating operators

In this section we present and recall some results concerning the bivariate C^2 quartic spline space $S_4^2(\Omega, \mathcal{T}_{m,n})$, where $\mathcal{T}_{m,n}$ is a uniform criss-cross triangulation of a rectangular domain $\Omega = [0, mh] \times [0, nh]$ (see Fig. 1(*a*)), and we propose some linear quasi-interpolating operators.

In particular here we consider the proper subspace of $S_4^2(\Omega, \mathcal{T}_{m,n})$ denoted by $S_4^2(\Omega, \mathcal{T}_{m,n}, X_1)$. It is generated by the $(m+4)(n+4)-4$ local spline functions $\{B_{1,\alpha}, \alpha \in \mathcal{A}\}$, where $\mathcal{A} = \{(i,j),\ -1 \le i \le m+2,\ -1 \le j \le n+2;\ (i,j) \ne (-1,-1), (m+2,-1), (-1,n+2), (m+2,n+2)\}$, obtained by dilation/translation of the quartic box spline B_1 (see Fig. 1(*b*)) defined by the set of direction vectors of $\mathbb{R}^2$ $X_1 = \{e_1, e_2, e_3, e_3, e_4, e_4\}$ with $e_1 = (1,0)$, $e_2 = (0,1)$, $e_3 = (1,1)$, $e_4 = (-1,1)$ (see [9, Chap. 11], [10,26]). Since B_1 is centred at the point $(\frac{1}{2}, \frac{5}{2})$, we define the scaled translates of B_1, $B_{1,\alpha}, \alpha \in \mathcal{A}$, in the following way:

$$B_{1,\alpha}(x,y) = B_{1,(i,j)}(x,y) = B_1\left(\frac{x}{h} - i + 1, \frac{y}{h} - j + 3\right),$$

whose supports are centred at the points $C_\alpha = C_{i,j} = \left((i - \frac{1}{2})h, (j - \frac{1}{2})h\right)$. The Bernstein-Bézier coefficients of B_1 are given in [26, Fig. 1].

We remark that the space $S_4^2(\Omega, \mathcal{T}_{m,n}, X_1)$ is a proper subspace of $S_4^{3,2}(\Omega, \mathcal{T}_{m,n})$ [26], where a spline $s \in S_4^{3,2}(\Omega, \mathcal{T}_{m,n})$ is a polynomial of degree 4 in each triangle and it is C^3 continuous on the rectangle grid segments $x - ih = 0$, $y - ih = 0$, and C^2 continuous on the diagonal grid segments $x - y - ih = 0$, $x + y - ih = 0$.

In the spline space $S_4^2(\Omega, \mathcal{T}_{m,n}, X_1)$ we construct linear quasi-interpolants

$$Q : C(\Omega) \longrightarrow S_4^2(\Omega, \mathcal{T}_{m,n}, X_1), \qquad Qf = \sum_{\alpha \in \mathcal{A}} \lambda_\alpha(f)\, B_{1,\alpha}.$$

The coefficient functionals $\left\{\lambda_\alpha,\ \alpha \in A\right\}$ can be of different kinds, see e.g. [11,21,22], and here we consider point QIs. Given a set of quasi-interpolation nodes $\left\{P_\alpha,\ \alpha \in D\right\}$, for a suitable set of indices D, the coefficient functionals have the form

$$\lambda_\alpha(f) = \sum_{\beta \in F_\alpha} \sigma_\alpha(\beta) f(P_\beta),$$

where the finite set of points $\left\{P_\beta,\ \beta \in F_\alpha\right\}$, $F_\alpha \subset D$, lies in some neighbourhood of the support Σ_α of $B_{1,\alpha}$ and such that $Qf \equiv f$ for all f in $\mathbb{P}_3$, the space of cubic polynomials. The points P_α, $\alpha \in D$, used in evaluating f are (see Fig. 1(*a*)) the vertices $A_{i,j} = (ih, jh)$, $i = 0, \ldots, m$, $j = 0, \ldots, n$ and the centres $M_{i,j} = (s_i, t_j)$, $i = 1, \ldots, m$, $j = 1, \ldots, n$ of squares, with $s_i = (i - \frac{1}{2})h$, $t_j = (j - \frac{1}{2})h$. We introduce the following notation $\bar{f}_{i,j} = f(M_{i,j})$ and $f_{i,j} = f(A_{i,j})$.

Different point QIs in such a spline space have been proposed in the literature [1,6,7,15,20,21,23,26] considering different set of QI nodes and here we propose the following ones:

1. $Q^1 f = \sum_{\alpha\in\mathcal{A}} \lambda^1_\alpha(f) B_{1,\alpha}$, with (see Fig. 2(*a*))

$$\begin{aligned}\lambda^1_{i,j}(f) = \;& \frac{61}{36}\bar f_{i,j} - \frac{85}{576}\left(\bar f_{i-1,j}+\bar f_{i+1,j}+\bar f_{i,j-1}+\bar f_{i,j+1}\right) - \frac{5}{144}\left(\bar f_{i-2,j}+\bar f_{i+2,j}+\bar f_{i,j-2}+\bar f_{i,j+2}\right)\\ &+\frac{5}{576}\left(\bar f_{i-3,j}+\bar f_{i+3,j}+\bar f_{i,j-3}+\bar f_{i,j+3}\right),\end{aligned}$$

2. $Q^2 f = \sum_{\alpha\in\mathcal{A}} \lambda^2_\alpha(f) B_{1,\alpha}$, with (see Fig. 2(*b*))

$$\begin{aligned}\lambda^2_{i,j}(f) = \;& \frac{25}{12}(f_{i-1,j-1}+f_{i-1,j}+f_{i,j}+f_{i,j-1})\\ &-\frac{25}{96}(f_{i-1,j+1}+f_{i,j+1}+f_{i+1,j-1}+f_{i+1,j}+f_{i-1,j-2}+f_{i-2,j-1}+f_{i-2,j}+f_{i,j-2})\\ &+\frac{5}{96}(f_{i-1,j+2}+f_{i,j+2}+f_{i,j-3}+f_{i+2,j-1}+f_{i+2,j}+f_{i-1,j-3}+f_{i-3,j-1}+f_{i-3,j})\\ &-\frac{25}{24}(\bar f_{i,j+1}+\bar f_{i,j-1}+\bar f_{i-1,j}+\bar f_{i+1,j})+\frac{5}{48}(\bar f_{i,j+2}+\bar f_{i+2,j}+\bar f_{i,j-2}+\bar f_{i-2,j})-\frac{23}{12}\bar f_{i,j},\end{aligned}$$

3. $Q^3 f = \sum_{\alpha\in\mathcal{A}} \lambda^3_\alpha(f) B_{1,\alpha}$, with (see Fig. 2(*c*))

$$\begin{aligned}\lambda^3_{i,j}(f) = \;& \frac{7}{12}\left(f_{i-1,j-1}+f_{i-1,j-1}+f_{i,j-1}+f_{i,j}\right)-\frac{5}{24}(f_{i-1,j+1}+f_{i,j+1}+f_{i+1,j-1}+f_{i+1,j})\\ &-\frac{5}{24}(f_{i-1,j-2}+f_{i-2,j-1}+f_{i-2,j}+f_{i,j-2})+\frac{1}{24}(f_{i-1,j-3}+f_{i,j-3}+f_{i-3,j-1}+f_{i-3,j})\\ &+\frac{1}{24}(f_{i-1,j+2}+f_{i,j+2}+f_{i+2,j-1}+f_{i+2,j}),\end{aligned}$$

4. $Q^4 f = \sum_{\alpha\in\mathcal{A}} \lambda^4_\alpha(f) B_{1,\alpha}$, with (see Fig. 2(*d*))

$$\begin{aligned}\lambda^4_{i,j}(f) = \;& \frac{125}{192}(f_{i-1,j}+f_{i-1,j-1}+f_{i,j}+f_{i,j-1})+\frac{13}{3072}(f_{i-3,j-3}+f_{i-3,j+2}+f_{i+2,j-3}+f_{i+2,j+2})\\ &-\frac{75}{256}(f_{i-1,j+1}+f_{i,j+1}+f_{i+1,j-1}+f_{i+1,j}+f_{i-1,j-2}+f_{i,j-2}+f_{i-2,j}+f_{i-2,j-1})\\ &-\frac{65}{3072}(f_{i+1,j+2}+f_{i+2,j+1}+f_{i+1,j-3}+f_{i+2,j-2}+f_{i-2,j+2}+f_{i-3,j+1}+f_{i-2,j-3}+f_{i-3,j-2})\\ &+\frac{15}{256}(f_{i-3,j}+f_{i-3,j-1}+f_{i+2,j}+f_{i+2,j-1}+f_{i,j-3}+f_{i,j+2}+f_{i-1,j-3}+f_{i-1,j+2})\\ &+\frac{325}{3072}(f_{i-2,j-2}+f_{i-2,j+1}+f_{i+1,j-2}+f_{i+1,j+1}),\end{aligned}$$

all exact on $\mathbb{P}_3$. They can be obtained by suitable discretisation of the Laplacian Δ in the differential QI exact on $\mathbb{P}_3$ (see [21,23])

$$\hat Q f = \sum_{\alpha\in\mathcal{A}} \hat\lambda_\alpha(f) B_{1,\alpha} \tag{2.1}$$

with

$$\hat\lambda_\alpha(f) = \left(f(C_\alpha) - \frac{5}{24}h^2\Delta f(C_\alpha)\right). \tag{2.2}$$

We remark that it is necessary to evaluate the function outside the domain Ω in order to construct the coefficient functionals for boundary spanning functions, i.e. spanning functions whose support is not completed included in Ω. In this paper we extend the triangulation outside Ω and another approach is the construction of suitable coefficient functionals for boundary generators (see e.g. [20] where specific boundary functionals are available, following the method proposed in [19] for quadratic splines).

Regarding the approximation properties of such operators (see e.g. [10,11,13]), we say that a QI Q has approximation order k if $\|f - Qf\|_\infty \le Ch^k$, $f \in C^k(\Omega)$, i.e. the maximum error is $O(h^k)$ for $h \to 0$, with an h-independent constant C. The maximum value of k we can obtain, that provides optimal approximation, is related to the polynomial reproduction properties of Q. Since the above mentioned QIs reproduce $\mathbb{P}_3$, they have the optimal approximation order 4. If the function f has a jump inside Ω, then we expect $\|f - Qf\|_\infty = O(h^0)$.

3. Nonlinear spline quasi-interpolating operators

In this section we modify the linear spline quasi-interpolants of Section 2, by applying WENO techniques (see e.g. [2,3,16,24]) for constructing nonlinear quasi-interpolants able to deal with piecewise smooth functions.

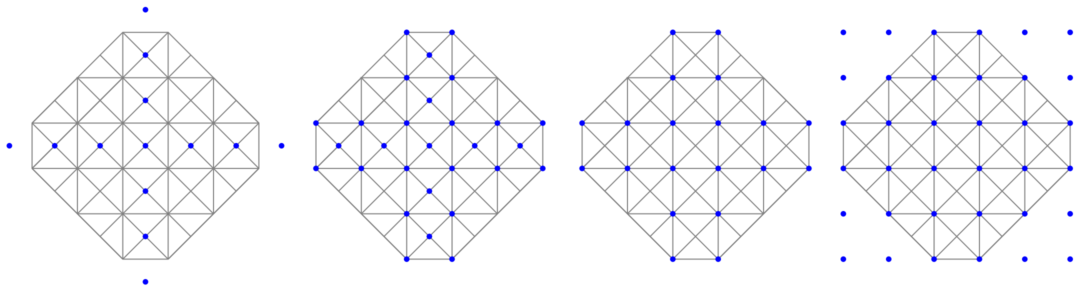

Fig. 2. Coefficient functionals $\lambda^k_{i,j}(f)$, $k=1,2,3,4$ for different point QIs.

Therefore, we consider the differential QI (2.1) with coefficient functional $\widehat{\lambda}_{i,j}(f)$ given in (2.2) and we assume to have different approximations of $\widehat{\lambda}_{i,j}(f)$ such that:

$$\mu(f)=\widehat{\lambda}_{i,j}(f)+O(h^p), \qquad \mu_l(f)=\widehat{\lambda}_{i,j}(f)+O(h^q),\ l=1,\dots,N, \tag{3.1}$$

where $p\ge q$, $p,\ q\in\mathbb{N}$, and $\mu(f)=\sum_{l=1}^N \gamma_l\mu_l(f)$, for suitable positive values γ_l, $l=1,\dots,N$. The WENO technique is applied to obtain an enhanced version of $\mu(f)$ which (essentially) does not produce oscillations. We define the quantities

$$\alpha_l(f)=\frac{\gamma_l}{(\epsilon+I_l(f))^2}, \qquad \omega_l(f)=\frac{\alpha_l(f)}{\sum_{l=1}^N\alpha_l(f)}, \quad l=1,\dots,N, \tag{3.2}$$

with $\epsilon=10^{-7}$ and $I_l(f)\ge 0$ is a smoothness indicator able to detect the region of discontinuity. Then, the nonlinear coefficient functional is

$$\mu^{\omega}(f)=\sum_{l=1}^N\omega_l(f)\mu_l(f). \tag{3.3}$$

If f is smooth, then $\mu^{\omega}(f)$ is as accurate as $\mu(f)$,

$$\mu^{\omega}(f)=\widehat{\lambda}_{i,j}(f)+O(h^p) \tag{3.4}$$

and if f has a discontinuity in the interval where the data used by $\mu(f)$ lie, but it is smooth in the area involved in the construction of at least one $\mu_l(f)$, then $\mu^{\omega}(f)$ is as precise as $\mu_l(f)$, i.e.

$$\mu^{\omega}(f)=\widehat{\lambda}_{i,j}(f)+O(h^q).$$

Now we apply this technique to the linear QIs of the previous section. For the operator Q^1 the method is slightly different with respect to the other three operators, because for Q^1 we apply the WENO technique separately in the two directions x and y. Since we can write $\lambda^1_{i,j}(f)$ in this way

$$\begin{aligned}\lambda^1_{i,j}(f)=\bar f_{i,j}&-\frac{5}{24}\left(\frac{1}{24}(-\bar f_{i-3,j}+4\,\bar f_{i-2,j}-5\,\bar f_{i-1,j}+2\,\bar f_{i,j})+\frac{22}{24}(\bar f_{i-1,j}-2\,\bar f_{i,j}+\bar f_{i+1,j})\right.\\ &\left.+\frac{1}{24}(2\,\bar f_{i,j}-5\,\bar f_{i+1,j}+4\,\bar f_{i+2,j}-\bar f_{i+3,j})\right)\\ &-\frac{5}{24}\left(\frac{1}{24}(-\bar f_{i,j-3}+4\,\bar f_{i,j-2}-5\,\bar f_{i,j-1}+2\,\bar f_{i,j})+\ \frac{22}{24}(\bar f_{i,j-1}-2\bar f_{i,j}+\bar f_{i,j+1})\right.\\ &\left.+\frac{1}{24}(2\,\bar f_{i,j}-5\,\bar f_{i,j+1}+4\,\bar f_{i,j+2}-\bar f_{i,j+3})\right)\\ =\bar f_{i,j}&-\frac{5}{24}\left(\gamma_1\lambda^{\ell j}_{i,j}(f)+\gamma_2\lambda^{cj}_{i,j}(f)+\gamma_3\lambda^{rj}_{i,j}(f)\right)-\frac{5}{24}\left(\gamma_1\lambda^{\ell i}_{i,j}(f)+\gamma_2\lambda^{ci}_{i,j}(f)+\gamma_3\lambda^{ri}_{i,j}(f)\right),\end{aligned} \tag{3.5}$$

where $\gamma_1=\gamma_3=\frac{1}{24}$, $\gamma_2=\frac{22}{24}$, applying the WENO strategy to the approximations of each directional derivative in (3.5), with

$$I^{\ell j}_{i,j}=\frac{1}{2}(\bar f_{i-3,j}-2\,\bar f_{i-2,j}+\bar f_{i-1,j})^2+\frac{1}{2}(\bar f_{i-2,j}-2\,\bar f_{i-1,j}+\bar f_{i,j})^2, \quad I^{cj}_{i,j}=(\bar f_{i-1,j}-2\,\bar f_{i,j}+\bar f_{i+1,j})^2,$$
$$I^{rj}_{i,j}=\frac{1}{2}(\bar f_{i,j}-2\,\bar f_{i+1,j}+\bar f_{i+2,j})^2+\frac{1}{2}(\bar f_{i+1,j}-2\,\bar f_{i+2,j}+\bar f_{i+3,j})^2,$$

and

$$I^{\ell i}_{i,j}=\frac{1}{2}(\bar f_{i,j-3}-2\,\bar f_{i,j-2}+\bar f_{i,j-1})^2+\frac{1}{2}(\bar f_{i,j-2}-2\,\bar f_{i,j-1}+\bar f_{i,j})^2,\quad I^{ci}_{i,j}=(\bar f_{i,j-1}-2\bar f_{i,j}+\bar f_{i,j+1})^2,$$
$$I^{ri}_{i,j}=\frac{1}{2}(\bar f_{i,j}-2\,\bar f_{i,j+1}+\bar f_{i,j+2})^2+\frac{1}{2}(\bar f_{i,j+1}-2\,\bar f_{i,j+2}+\bar f_{i,j+3})^2,$$

we obtain (consider (3.2) and (3.3) for the approximation of each directional derivative)

$$\omega^1_{i,j}(f)=\bar f_{i,j}-\frac{5}{24}\left(\omega^{\ell j}_{i,j}\lambda^{\ell j}_{i,j}(f)+\omega^{cj}_{i,j}\lambda^{cj}_{i,j}(f)+\omega^{rj}_{i,j}\lambda^{rj}_{i,j}(f)\right)-\frac{5}{24}\left(\omega^{\ell i}_{i,j}\lambda^{\ell i}_{i,j}(f)+\omega^{ci}_{i,j}\lambda^{ci}_{i,j}(f)+\omega^{ri}_{i,j}\lambda^{ri}_{i,j}(f)\right).$$

Moreover, we have (see (3.1))

$$\lambda^1_{i,j}(f)=\widehat\lambda_{i,j}(f)+O(h^4),$$
$$\lambda^{pi}_{i,j}(f)=\frac{\partial^2 f}{\partial y^2}(C_\alpha)+O(h^4),\quad \lambda^{pj}_{i,j}(f)=\frac{\partial^2 f}{\partial x^2}(C_\alpha)+O(h^4),\qquad p=\ell,c,r.$$

For the other operators, we can write them in the following ways:

$$\begin{aligned}
\lambda^2_{i,j}(f)=&\frac{1}{4}\Big(\frac{5}{72}(f_{i-1,j-1}+f_{i,j})-\frac{125}{288}(f_{i-1,j+1}+f_{i-2,j})+\frac{25}{288}(f_{i-1,j+2}+f_{i-3,j})\\
&\quad+\frac{125}{48}f_{i-1,j}-\frac{7}{288}(f_{i,j+2}+f_{i-3,j-1})+\frac{35}{288}(f_{i,j+1}+f_{i-2,j-1})-\frac{35}{144}f_{i,j-1}\\
&\quad+\frac{1}{9}(\bar f_{i-2,j}+\bar f_{i,j+2})-\frac{10}{9}(\bar f_{i,j+1}+\bar f_{i-1,j})+\bar f_{i,j})\Big)\\
&+\frac{1}{4}\Big(\frac{5}{72}(f_{i-1,j}+f_{i,j-1})-\frac{125}{288}(f_{i-1,j-2}+f_{i-2,j-1})+\frac{25}{288}(f_{i-3,j-1}+f_{i-1,j-3})\\
&\quad+\frac{125}{48}f_{i-1,j-1}-\frac{7}{288}(f_{i,j-3}+f_{i-3,j})+\frac{35}{288}(f_{i,j-2}+f_{i-2,j})-\frac{35}{144}f_{i,j}\\
&\quad+\frac{1}{9}(\bar f_{i,j-2}+\bar f_{i-2,j})-\frac{10}{9}(\bar f_{i-1,j}+\bar f_{i,j-1})+\bar f_{i,j}\Big)\\
&+\frac{1}{4}\Big(\frac{5}{72}(f_{i-1,j}+f_{i,j-1})-\frac{125}{288}(f_{i,j+1}+f_{i+1,j})+\frac{25}{288}(f_{i,j+2}+f_{i+2,j})\\
&\quad+\frac{125}{48}f_{i,j}-\frac{7}{288}(f_{i-1,j+2}+f_{i+2,j-1})+\frac{35}{288}(f_{i-1,j+1}+f_{i+1,j-1})-\frac{35}{144}f_{i-1,j-1}\\
&\quad+\frac{1}{9}(\bar f_{i,j+2}+\bar f_{i+2,j})-\frac{10}{9}(\bar f_{i,j+1}+\bar f_{i+1,j})+\bar f_{i,j}\Big)\\
&+\frac{1}{4}\Big(\frac{5}{72}(f_{i-1,j-1}+f_{i,j}-\frac{125}{288}(f_{i+1,j-1}+f_{i,j-2})+\frac{25}{288}(f_{i+2,j-1}+f_{i,j-3})\\
&\quad+\frac{125}{48}f_{i,j-1}-\frac{7}{288}(f_{i-1,j-3}+f_{i+2,j})+\frac{35}{288}(f_{i-1,j-2}+f_{i+1,j})-\frac{35}{144}f_{i-1,j}\\
&\quad+\frac{1}{9}(\bar f_{i+2,j}+\bar f_{i,j-2})-\frac{10}{9}(\bar f_{i,j-1}+\bar f_{i+1,j})+\bar f_{i,j}\Big)\\
=&\frac{1}{4}\lambda^{2\ell t}_{i,j}(f)+\frac{1}{4}\lambda^{2\ell b}_{i,j}(f)+\frac{1}{4}\lambda^{2rt}_{i,j}(f)+\frac{1}{4}\lambda^{2rb}_{i,j}(f),\\
\lambda^3_{i,j}(f)=&\frac{1}{4}\Big(\frac{17}{12}f_{i-1,j}+\frac{7}{12}(f_{i-1,j-1}+f_{i,j})-\frac{1}{4}f_{i,j-1}-\frac{5}{12}(f_{i-1,j+1}+f_{i,j+1}-f_{i-2,j-1}-f_{i-2,j})\\
&\quad+\frac{1}{12}(f_{i-3,j-1}+f_{i-3,j}+f_{i-1,j+2}+f_{i,j+2})\Big)\\
&+\frac{1}{4}\Big(\frac{17}{12}f_{i,j}+\frac{7}{12}(f_{i-1,j}+f_{i,j-1})-\frac{1}{4}f_{i-1,j-1}-\frac{5}{12}(f_{i-1,j+1}+f_{i,j+1}+f_{i+1,j-1}+f_{i+1,j})\\
&\quad+\frac{1}{12}(f_{i+2,j-1}+f_{i+2,j}+f_{i-1,j+2}+f_{i,j+2})\Big)\\
&+\frac{1}{4}\Big(\frac{17}{12}f_{i-1,j-1}+\frac{7}{12}(f_{i-1,j}+f_{i,j-1})-\frac{1}{4}f_{i,j}-\frac{5}{12}(f_{i-1,j-2}+f_{i,j-2}+f_{i-2,j-1}+f_{i-2,j})\\
&\quad+\frac{1}{12}(f_{i-3,j-1}+f_{i-3,j}+f_{i-1,j-3}+f_{i,j-3})\Big)\\
&+\frac{1}{4}\Big(\frac{17}{12}f_{i,j-1}+\frac{7}{12}(f_{i,j}+f_{i-1,j-1})-\frac{1}{4}f_{i-1,j}-\frac{5}{12}(f_{i+1,j-1}+f_{i+1,j}+f_{i-1,j-2}+f_{i,j-2})\\
&\quad+\frac{1}{12}(f_{i,j-3}+f_{i+2,j-1}+f_{i+2,j}+f_{i-1,j-3})\Big)\\
=&\frac{1}{4}\lambda^{3\ell t}_{i,j}(f)+\frac{1}{4}\lambda^{3rt}_{i,j}(f)+\frac{1}{4}\lambda^{3\ell b}_{i,j}(f)+\frac{1}{4}\lambda^{3rb}_{i,j}(f),\\
\lambda^4_{i,j}(f)=&\frac{1}{4}\Big(-\frac{25}{256}f_{i,j}+\frac{175}{768}(f_{i,j-1}+f_{i-1,j})+\frac{575}{256}f_{i-1,j-1}-\frac{125}{768}(f_{i,j-2}+f_{i-2,j})
\end{aligned}$$

$$
\begin{aligned}
&-\frac{65}{768}(f_{i-2,j-3}+f_{i-3,j-2})+\frac{25}{768}(f_{i-3,j}+f_{i,j-3})+\frac{155}{768}(f_{i-1,j-3}+f_{i-3,j-1})\\
&-\frac{775}{768}(f_{i-1,j-2}+f_{i-2,j-1})+\frac{13}{768}f_{i-3,j-3}+\frac{325}{768}f_{i-2,j-2}\Big)\\
&+\frac{1}{4}\Big(-\frac{25}{256}f_{i-1,j-1}+\frac{175}{768}(f_{i,j-1}+f_{i-1,j})+\frac{575}{256}f_{i,j}-\frac{125}{768}(f_{i-1,j+1}+f_{i+1,j-1})\\
&-\frac{65}{768}(f_{i+2,j+1}+f_{i+1,j+2})+\frac{25}{768}(f_{i-1,j+2}+f_{i+2,j-1})+\frac{155}{768}(f_{i,j+2}+f_{i+2,j})\\
&-\frac{775}{768}(f_{i,j+1}+f_{i+1,j})+\frac{13}{768}f_{i+2,j+2}+\frac{325}{768}f_{i+1,j+1}\Big)\\
&+\frac{1}{4}\Big(-\frac{25}{256}f_{i,j-1}+\frac{175}{768}(f_{i,j}+f_{i-1,j-1})+\frac{575}{256}f_{i-1,j}-\frac{125}{768}(f_{i,j+1}+f_{i-2,j-1})\\
&-\frac{65}{768}(f_{i-2,j+2}+f_{i-3,j+1})+\frac{25}{768}(f_{i,j+2}+f_{i-3,j-1})+\frac{155}{768}(f_{i-3,j}+f_{i-1,j+2})\\
&-\frac{775}{768}(f_{i-1,j+1}+f_{i-2,j})+\frac{13}{768}f_{i-3,j+2}+\frac{325}{768}f_{i-2,j+1}\Big)\\
&+\frac{1}{4}\Big(-\frac{25}{256}f_{i-1,j}+\frac{175}{768}(f_{i-1,j-1}+f_{i,j})+\frac{575}{256}f_{i,j-1}-\frac{125}{768}(f_{i-1,j-2}+f_{i+1,j})\\
&-\frac{65}{768}(f_{i+1,j-3}+f_{i+2,j-2})+\frac{25}{768}(f_{i-1,j-3}+f_{i+2,j})+\frac{155}{768}(f_{i,j-3}+f_{i+2,j-1})\\
&-\frac{775}{768}(f_{i+1,j-1}+f_{i,j-2})+\frac{13}{768}f_{i+2,j-3}+\frac{325}{768}f_{i+1,j-2}\Big)\\
&=\frac{1}{4}\lambda^{4\ell b}_{i,j}(f)+\frac{1}{4}\lambda^{4rt}_{i,j}(f)+\frac{1}{4}\lambda^{4\ell t}_{i,j}(f)+\frac{1}{4}\lambda^{4rb}_{i,j}(f),
\end{aligned}
$$

and we can observe that (see (3.1))

$$
\begin{aligned}
&\lambda^{k}_{i,j}(f)=\widehat{\lambda}_{i,j}(f)+O(h^4), \qquad k=2,3,4,\\
&\lambda^{k\ell b}_{i,j}(f),\ \lambda^{krt}_{i,j}(f),\ \lambda^{krb}_{i,j}(f),\ \lambda^{k\ell t}_{i,j}(f)=\widehat{\lambda}_{i,j}(f)+O(h^4), \qquad k=2,3,4.
\end{aligned}
\tag{3.6}
$$

Now we apply the WENO technique. First of all we have $\gamma_1=\gamma_2=\gamma_3=\gamma_4=\frac{1}{4}$. Regarding the smoothness indicators, we choose the following ones:

- for Q^2 and Q^3

$$
I^{rt}_{i,j}=\frac{1}{4}\left[\sum_{l=j-1,j}(f_{i-1,l}-3f_{i,l}+3f_{i+1,l}-f_{i+2,l})^2+\sum_{l=i-1,i}(f_{l,j-1}-3f_{l,j}+3f_{l,j+1}-f_{l,j+2})^2\right]
$$

  and the other three ones $I^{rb}_{i,j}$, $I^{\ell t}_{i,j}$, $I^{\ell b}_{i,j}$ by symmetry,
- for Q^4

$$
I^{rt}_{i,j}=\frac{1}{8}\left[\sum_{l=j-1,j,j+1,j+2}(f_{i-1,l}-3f_{i,l}+3f_{i+1,l}-f_{i+2,l})^2+\sum_{l=i-1,i,i+1,i+2}(f_{l,j-1}-3f_{l,j}+3f_{l,j+1}-f_{l,j+2})^2\right]
$$

  and the other three ones $I^{rb}_{i,j}$, $I^{\ell t}_{i,j}$, $I^{\ell b}_{i,j}$ by symmetry.

We compute the WENO quantities appearing in (3.2) as above explained and, by using (3.3), we obtain the nonlinear coefficient functionals

$$
\omega^{k}_{i,j}(f)=\omega^{k\ell t}_{i,j}(f)\lambda^{k\ell t}_{i,j}(f)+\omega^{k\ell b}_{i,j}(f)\lambda^{k\ell b}_{i,j}(f)+\omega^{krt}_{i,j}(f)\lambda^{krt}_{i,j}(f)+\omega^{krb}_{i,j}(f)\lambda^{krb}_{i,j}(f), \qquad k=2,3,4.
$$

In order to study the theoretical properties of the new operators, we define the following domains

$$
\Omega^{+}_{\mu,\nu}:=[x_\mu,x_m]\times[y_\nu,y_n], \qquad \Omega^{-}_{\mu,\nu}:=[x_0,x_\mu]\times[y_0,y_\nu],
$$

Theorem 1. *If we define*

$$
W^k f=\sum_{\alpha\in A}\omega^{k}_{\alpha}(f)B_{1,\alpha}, \qquad k=1,2,3,4,
$$

the following results hold:

1. *W^k is exact on the space $\mathbb{P}_3$.*
2. *If f is smooth, then $\|f-W^k f\|_\infty=O(h^4)$.*

3. *If f has a discontinuity across the square $(s_\mu, s_{\mu+1})\times(t_\nu, t_{\nu+1})$, and it is smooth on $\Omega^+_{\mu+1,\nu+1}$ and $\Omega^-_{\mu-1,\nu-1}$, then $\left\|f - W^1 f\right\|_{\Omega^+_{\mu+2,\nu+2},\infty} = O(h^4)$, $\left\|f - W^1 f\right\|_{\Omega^-_{\mu-2,\nu-2},\infty} = O(h^4)$.*

   If f has a discontinuity across the square $(x_{\mu-1}, x_\mu)\times(y_{\nu-1}, y_\nu)$, and it is smooth on $\Omega^+_{\mu,\nu}$ and $\Omega^-_{\mu-1,\nu-1}$, then $\|f - W^k f\|_{\Omega^+_{\mu+2,\nu+2},\infty} = O(h^4)$, $\|f - W^k f\|_{\Omega^-_{\mu-3,\nu-3},\infty} = O(h^4)$, for $k = 2, 3, 4$.

Proof. The theorem is proved by following the logical scheme used in [5]. If the function f is smooth, the statement 2 follows by the fact that the differential QI operator has approximation order 4, i.e. $\left\|f - \widehat{Q}f\right\|_\infty = O(h^4)$, by (3.4) and (3.6). Moreover, for $k = 1, 2, 3, 4$, the parts into which $\lambda^k_{i,j}(f)$ and $\omega^k_{i,j}(f)$ have been subdivided guarantee $W^k p = p$, $\forall p \in \mathbb{P}_3$, so the statement 1 is proved.

In order to prove statement 3, taking into account the definition of $\lambda^1_{i,j}(f)$ (see Section 2 and Fig. 2(*a*)), if f has a discontinuity across the square $(s_\mu, s_{\mu+1}) \times (t_\nu, t_{\nu+1})$, then there are 24 spanning functions $B_{1,(i,j)}$ with support overlapping this interval and only starting from $\Omega^+_{\mu+2,\nu+2}$ (similarly for $\Omega^-_{\mu-2,\nu-2}$) we are able to construct the spline $W^1 f$ using information only on one side of the discontinuity.

Analogously, if f has a discontinuity in $(x_{\mu-1}, x_\mu) \times (y_{\nu-1}, y_\nu)$, taking into account the definition of $\lambda^k_{i,j}(f)$, $k = 2, 3, 4$ (see Section 2 and Fig. 2), there are 21 spanning functions $B_{1,(i,j)}$ with support overlapping the considered interval and only starting from $\Omega^+_{\mu+2,\nu+2}$ (similarly for $\Omega^-_{\mu-3,\nu-3}$) we are able to construct the spline $W^k f$, $k = 2, 3, 4$ using information only on one side of the discontinuity. □

Remark 2. If the discontinuity is across the square $(s_\mu, s_{\mu+1}) \times (t_\nu, t_{\nu+1})$, the region affected by the discontinuity in $Q^1 f$ is $[x_{\mu-5}, x_{\mu+5}] \times [y_{\nu-5}, y_{\nu+5}]$. If the discontinuity is across the square $(x_{\mu-1}, x_\mu) \times (y_{\nu-1}, y_\nu)$, the region affected by the discontinuity in $Q^k f$, $k = 2, 3, 4$ is $[x_{\mu-5}, x_{\mu+4}] \times [y_{\nu-5}, y_{\nu+4}]$. The results follow from the definition of $\lambda^k_{i,j}(f)$, $k = 1, \ldots, 4$ (see Fig. 2) and from the fact that support of $B_{1,(i,j)}$ is contained in the square $[x_{i-3}, x_{i+2}] \times [y_{j-3}, y_{j+2}]$. In the rest of the domain, the approximation order 4 is maintained.

4. Numerical and graphical results

In this section we provide some numerical and graphical results in order to confirm the theoretical ones obtained in Theorem 1.

In all cases we compare the linear operators, $\{Q^k\}^4_{k=1}$, with the nonlinear ones, $\{W^k\}^4_{k=1}$, presented in Section 3.

We have also tested the reproduction properties of all quasi-interpolants and the results are in line with the theoretical ones reported in Theorem 1 and Remark 2.

Moreover, regarding the boundary of the domain Ω, we have extended the triangulation outside Ω in order to be able to evaluate the test functions and construct the coefficient functionals associated with boundary generators.

4.1. Test 1

We consider the piecewise smooth function (see Fig. 3)

$$f(x, y) = \begin{cases} \exp(x + y) & \text{if } \ y < 0.5 \\ \exp(x^2 + y^2) + 10 & \text{elsewhere} \end{cases}, \ (x, y) \in [0, 1] \times [0, 1]$$

and we compare the nonlinear quasi-interpolants in different sub-domains, in order to verify the theoretical results of Section 3. We compute the maximum absolute errors

$$E^{Q^k} f := \max_{(u,v)\in G} |f(u, v) - Q^k f(u, v)|, \quad E^{W^k} f := \max_{(u,v)\in G} |f(u, v) - W^k f(u, v)|,$$

and the corresponding numerical convergence orders, O^{Q^k}, O^{W^k}, $k = 1, 2, 3, 4$, for increasing values of m and n, using a 300×150 uniform rectangular grid G of evaluation points. In Table 1 we report the maximum absolute error in $[0, 1] \times \left[(\frac{n}{2} + 2)h, 1\right]$. We consider also the linear operators, for which we expect an error $O(h^0)$. We recall that in $[0, 1] \times \left[(\frac{n}{2} + 1)h, 1\right]$ all the operators Q^k, W^k, $k = 1, 2, 3, 4$ have an error $O(h^0)$.

Moreover, in order to recover all the theoretical results in Theorem 1 and Remark 2, we compute the maximum absolute error in $[0, 1] \times \left[(\frac{n}{2} + \beta)h, 1\right]$, with $\beta = 4, 5$. The corresponding results are reported in Tables 2, 3, respectively. Taking into account the location of the discontinuity, the numerical results confirm the theoretical ones. It is observed that we obtain $O(h^4)$ with the operators $\{W^k\}^4_{k=1}$ and $O(h^0)$ with the $\{Q^k\}^4_{k=1}$ in $[0, 1] \times \left[(\frac{n}{2} + \beta)h, 1\right]$ for $\beta = 2$. We also see that we obtain $O(h^4)$ with $\{Q^k\}^4_{k=2}$ when $\beta = 4$ and also with Q^1 when $\beta = 5$.

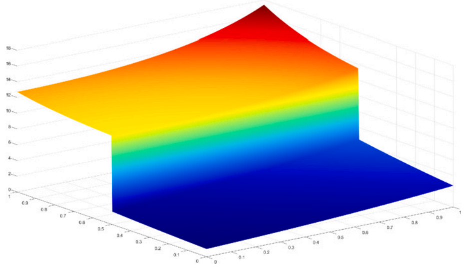

Fig. 3. The graphs of $f(x, y)$.

Table 1
Test 1 – Maximum absolute errors and numerical convergence order in $[0,1,] \times \left[(\frac{n}{2}+2)h, 1\right]$.

n	$E^{Q^1} f$	O^{Q^1}	$E^{Q^2} f$	O^{Q^2}	$E^{Q^3} f$	O^{Q^3}	$E^{Q^4} f$	O^{Q^4}
8	1.46(−01)		4.82(−01)		2.39(−01)		2.39(−01)	
16	1.46(−01)	-	4.85(−01)	-	2.40(−01)	-	2.40(−01)	-
32	1.46(−01)	-	4.84(−01)	-	2.39(−01)	-	2.39(−01)	-
64	1.46(−01)	-	4.84(−01)	-	2.34(−01)	-	2.34(−01)	-
128	1.46(−01)	-	4.15(−01)	-	2.34(−01)	-	2.34(−01)	-
256	1.46(−01)	-	3.76(−01)	-	2.34(−01)	-	2.34(−01)	-
n	$E^{W^1} f$	O^{W^1}	$E^{W^2} f$	O^{W^2}	$E^{W^3} f$	O^{W^3}	$E^{W^4} f$	O^{W^4}
8	8.86(−03)		2.93(−03)		5.24(−03)		9.56(−03)	
16	5.25(−04)	4.1	4.00(−04)	2.9	6.16(−04)	3.1	8.50(−04)	3.5
32	3.69(−05)	3.8	3.72(−05)	3.4	5.31(−05)	3.5	7.02(−05)	3.6
64	2.35(−06)	4.0	2.30(−06)	4.0	3.26(−06)	4.0	4.33(−06)	4.0
128	1.49(−07)	4.0	1.43(−07)	4.0	2.03(−07)	4.0	2.70(−07)	4.0
256	9.24(−09)	4.0	8.92(−09)	4.0	1.27(−08)	4.0	1.69(−08)	4.0

Table 2
Test 1 – Maximum absolute errors and numerical convergence order in $[0,1,] \times \left[(\frac{n}{2}+4)h, 1\right]$.

n	$E^{Q^1} f$	O^{Q^1}	$E^{Q^2} f$	O^{Q^2}	$E^{Q^3} f$	O^{Q^3}	$E^{Q^4} f$	O^{Q^4}
8	1.24(−02)		5.33(−02)		1.90(−02)		9.56(−02)	
16	3.57(−03)	-	2.82(−03)	4.2	9.11(−04)	4.4	8.50(−03)	3.5
32	3.49(−03)	-	1.69(−04)	4.1	5.31(−05)	4.1	7.02(−05)	3.6
64	3.49(−03)	-	1.05(−05)	4.0	3.26(−06)	4.0	4.33(−06)	4.0
128	3.49(−03)	-	6.52(−07)	4.0	2.03(−07)	4.0	2.70(−07)	4.0
256	3.49(−03)	-	4.07(−08)	4.0	1.27(−08)	4.0	1.69(−08)	4.0
n	$E^{W^1} f$	O^{W^1}	$E^{W^2} f$	O^{W^2}	$E^{W^3} f$	O^{W^3}	$E^{W^4} f$	O^{W^4}
8	8.86(−03)		2.58(−03)		5.24(−03)		9.56(−03)	
16	5.25(−04)	4.1	4.00(−04)	2.7	6.16(−04)	3.1	8.50(−04)	3.5
32	3.69(−05)	3.8	3.72(−05)	3.4	5.31(−05)	3.5	7.02(−05)	3.6
64	2.35(−06)	4.0	2.29(−06)	4.0	3.26(−06)	4.0	4.33(−06)	4.0
128	1.49(−07)	4.0	1.43(−07)	4.0	2.03(−07)	4.0	2.70(−07)	4.0
256	9.24(−09)	4.0	8.92(−09)	4.0	1.27(−08)	4.0	1.69(−08)	4.0

Table 3
Test 1 – Maximum absolute errors and numerical convergence order in $[0,1,] \times \left[(\frac{n}{2}+5)h, 1\right]$.

n	$E^{Q^1} f$	O^{Q^1}	$E^{Q^2} f$	O^{Q^2}	$E^{Q^3} f$	O^{Q^3}	$E^{Q^4} f$	O^{Q^4}
16	5.99(−04)		2.82(−03)	-	9.11(−04)	-	1.18(−03)	-
32	3.78(−05)	4.0	1.69(−04)	4.1	5.31(−05)	4.1	7.02(−05)	4.0
64	2.37(−06)	4.0	1.05(−05)	4.0	3.26(−06)	4.0	4.33(−06)	4.0
128	1.49(−07)	4.0	6.52(−07)	4.0	2.03(−07)	4.0	2.70(−07)	4.0
256	9.25(−09)	4.0	4.07(−08)	4.0	1.27(−08)	4.0	1.69(−08)	4.0
n	$E^{W^1} f$	O^{W^1}	$E^{W^2} f$	O^{W^2}	$E^{W^3} f$	O^{W^3}	$E^{W^4} f$	O^{W^4}
16	5.25(−04)	-	4.00(−04)	-	6.16(−04)	-	8.50(−04)	-
32	3.69(−05)	3.8	3.72(−05)	3.4	5.31(−05)	3.5	7.02(−05)	3.6
64	2.35(−06)	4.0	2.29(−06)	4.0	3.26(−06)	4.0	4.33(−06)	4.0
128	1.49(−07)	4.0	1.43(−07)	4.0	2.03(−07)	4.0	2.70(−07)	4.0
256	9.24(−09)	4.0	8.92(−09)	4.0	1.27(−08)	4.0	1.69(−08)	4.0

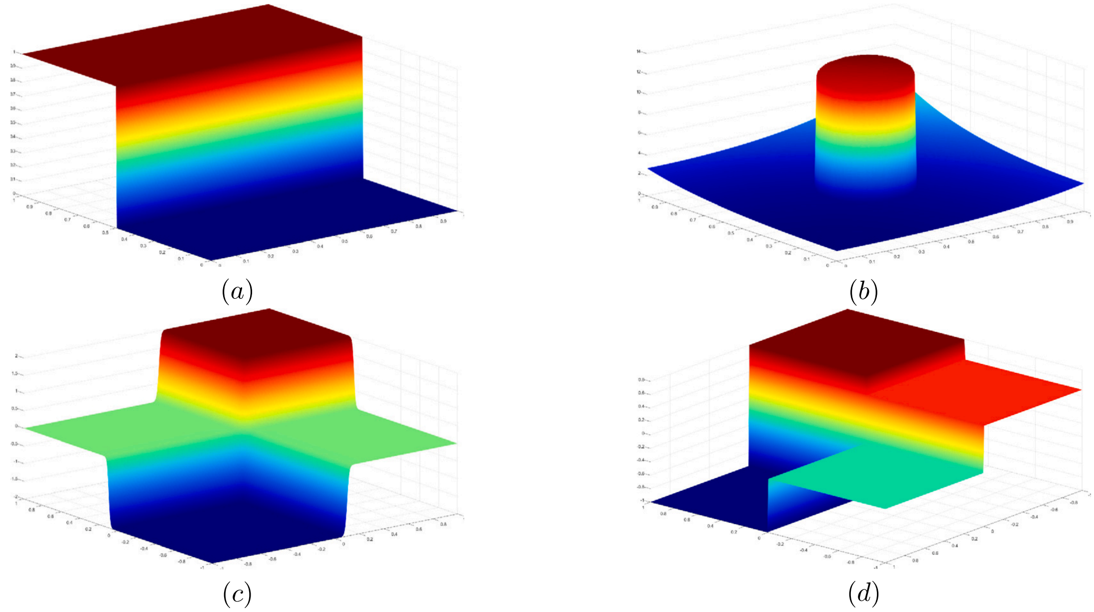

Fig. 4. The graphs of (a) $g(x, y)$, (b) $h(x, y)$, (c) $z(x, y)$ and (d) $u(x, y)$.

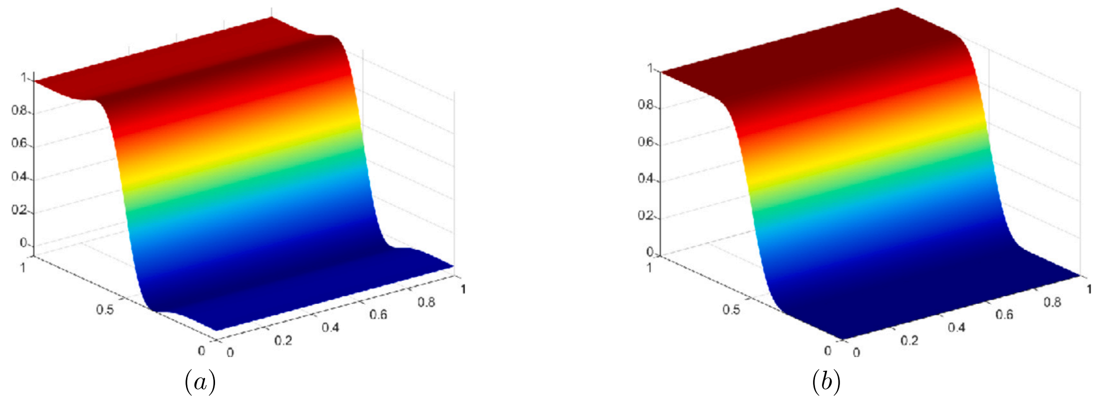

Fig. 5. The graphs of (a) $Q^1 g(x, y)$ and (b) $W^1 g(x, y)$ with $m = n = 8$.

4.2. Test 2

Now we propose some graphical results to confirm the reduction of the Gibbs phenomenon using the WENO technique. We compare all the quasi-interpolants proposed in the paper from the graphical point of view, considering the following functions:

- the step function shown in Fig. 4(a)

$$g(x, y) = \begin{cases} 0 & \text{if } y < \frac{1}{2} \\ 1 & \text{elsewhere} \end{cases}, \ (x, y) \in [0, 1] \times [0, 1],$$

- the piecewise smooth function shown in Fig. 4(b)

$$h(x, y) = \begin{cases} \exp(x + y) + 10 & \text{if } x^2 + y^2 < 0.025 \\ \exp(x^2 + y^2) & \text{elsewhere} \end{cases}, \ (x, y) \in [0, 1] \times [0, 1],$$

- the smooth function with a steep gradient shown in Fig. 4(c)

$$z(x, y) = \tanh(60x - 6) + \tanh(60y - 6), \ (x, y) \in [-1, 1] \times [-1, 1],$$

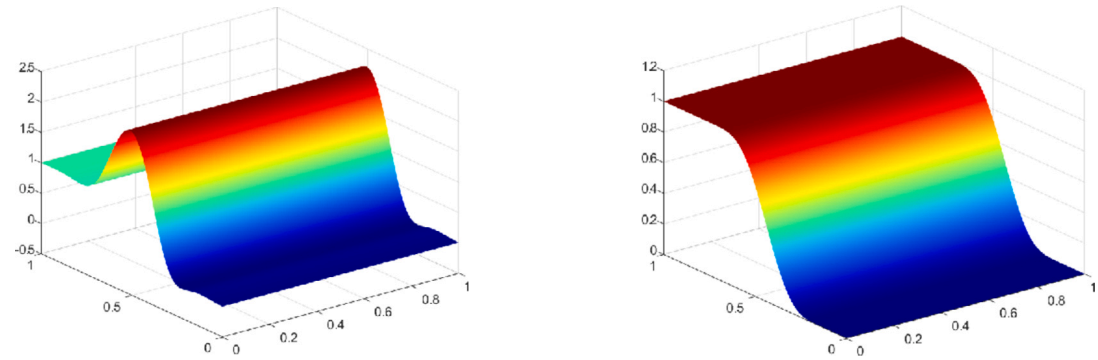

(a) (b)

Fig. 6. The graphs of (a) $Q^2 g(x, y)$ and (b) $W^2 g(x, y)$ with $m = n = 8$.

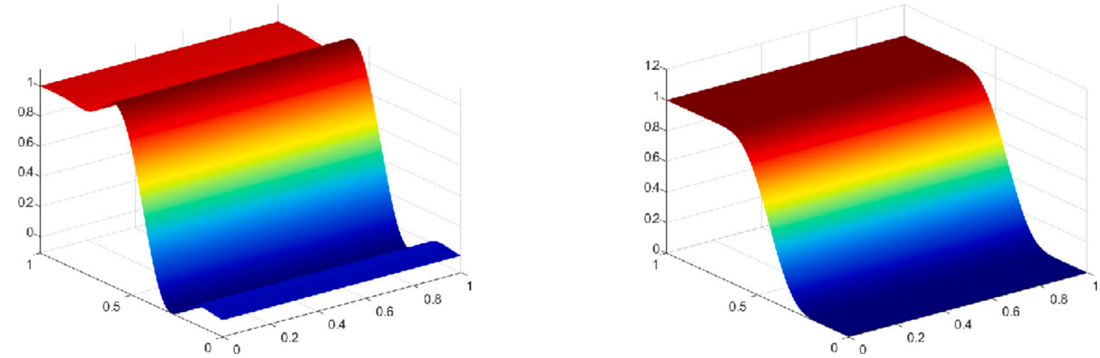

(a) (b)

Fig. 7. The graphs of (a) $Q^3 g(x, y)$ and (b) $W^3 g(x, y)$ with $m = n = 8$.

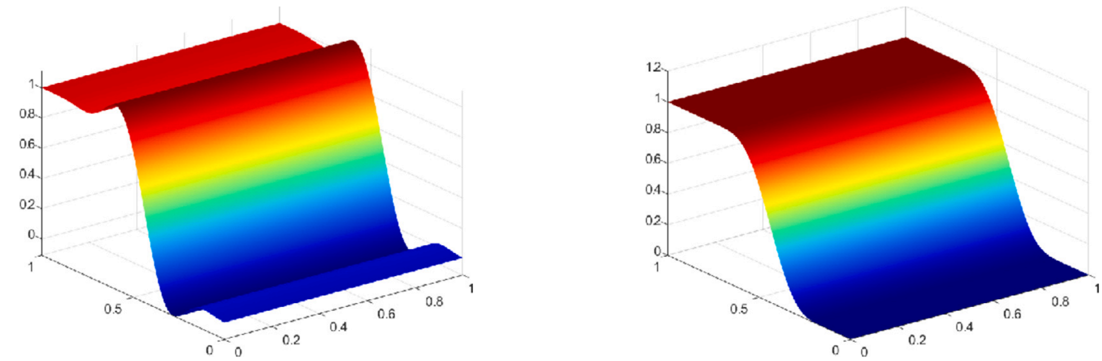

(a) (b)

Fig. 8. The graphs of (a) $Q^4 g(x, y)$ and (b) $W^4 g(x, y)$ with $m = n = 8$.

- the initial condition of a problem of conservation laws (see [17, Section 4.1]) shown in Fig. 4(d))

$$u(x,y) = \begin{cases} -1 & \text{if } x \geq 0,\ y \geq 0 \\ -0.2 & \text{if } x < 0,\ y \geq 0 \\ 0.5 & \text{if } x < 0,\ y < 0 \\ 0.8 & \text{if } x \geq 0,\ y < 0 \end{cases}, \ (x,y) \in [-1,1] \times [-1,1],$$

For each test function, for different values of m and n reported in the corresponding figure captions, we construct, evaluate and plot the eight spline quasi-interpolating surfaces using a 200×200 uniform grid of evaluation points.

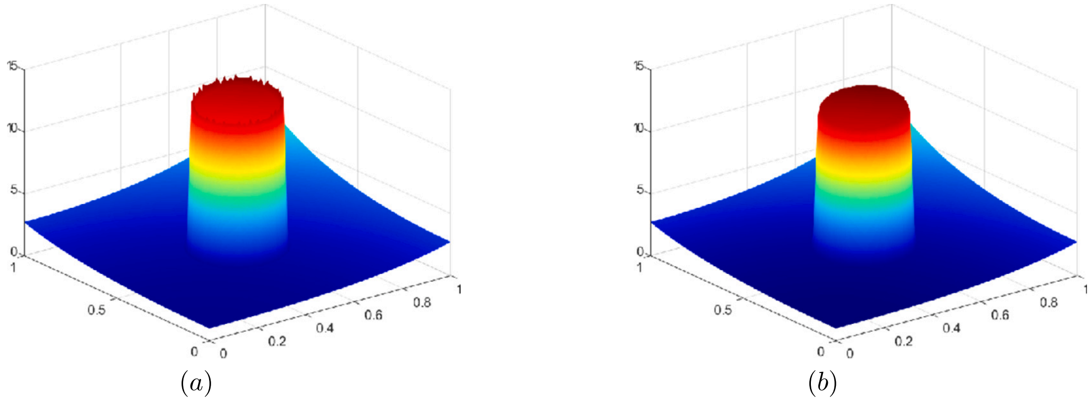

Fig. 9. The graphs of (a) $Q^1 h(x, y)$ and (b) $W^1 h(x, y)$ with $m = n = 128$.

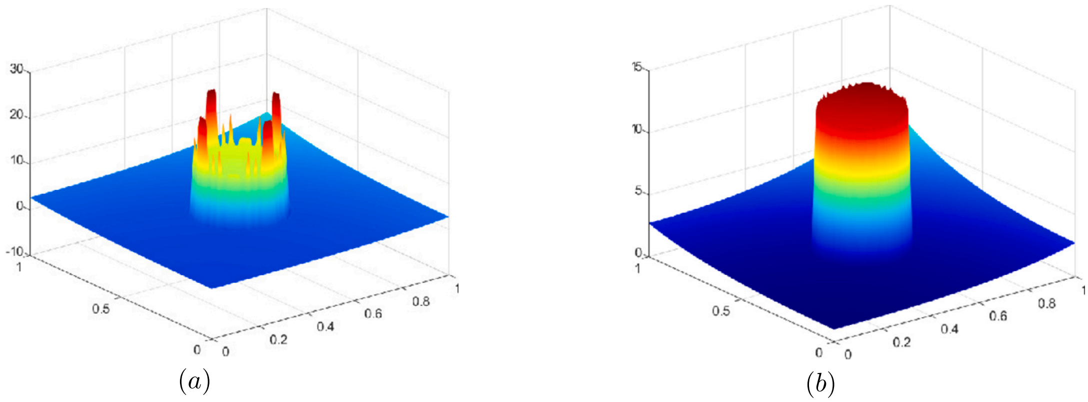

Fig. 10. The graphs of (a) $Q^2 h(x, y)$ and (b) $W^2 h(x, y)$ with $m = n = 128$.

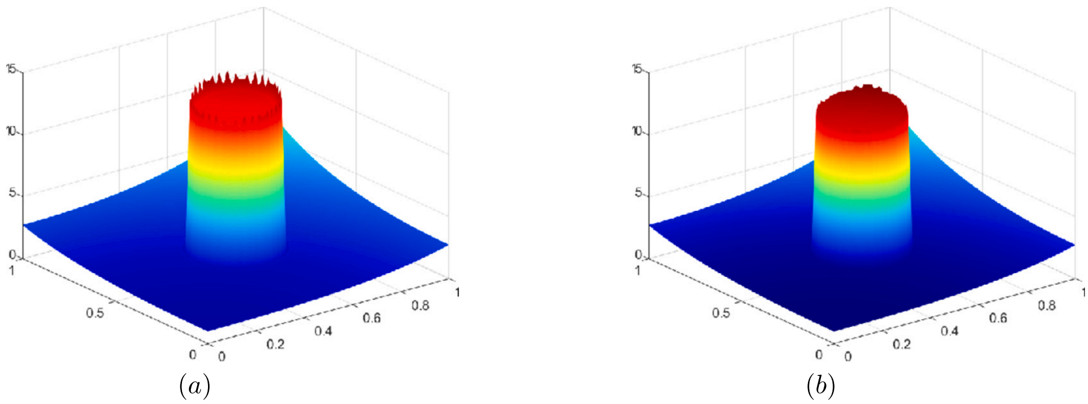

Fig. 11. The graphs of (a) $Q^3 h(x, y)$ and (b) $W^3 h(x, y)$ with $m = n = 128$.

Although the function $z(x, y)$ does not present a discontinuity like the other functions, in fact it has a steep gradient, it also presents the Gibbs phenomenon when reconstructed with linear operators. Indeed, we know that the Gibbs phenomenon is understood as those oscillations produced when trying to approximate a function with jumps, however, as remarked in [12], when few quasi-interpolation nodes are used, a smooth function with a steep gradient causes a similar effect to that of a jump function and we have used the expression "Gibbs phenomenon" in this extended sense.

We see that with the standard linear quasi-interpolants Q^k, $k = 1, 2, 3, 4$ we always obtain the Gibbs phenomenon (see Figs. 5–20(a)). Besides, we can observe that using the nonlinear quasi-interpolants W^k, $k = 1, 2, 3, 4$ (see Figs. 5–20(b)) the Gibbs phenomenon is not present, as we expected.

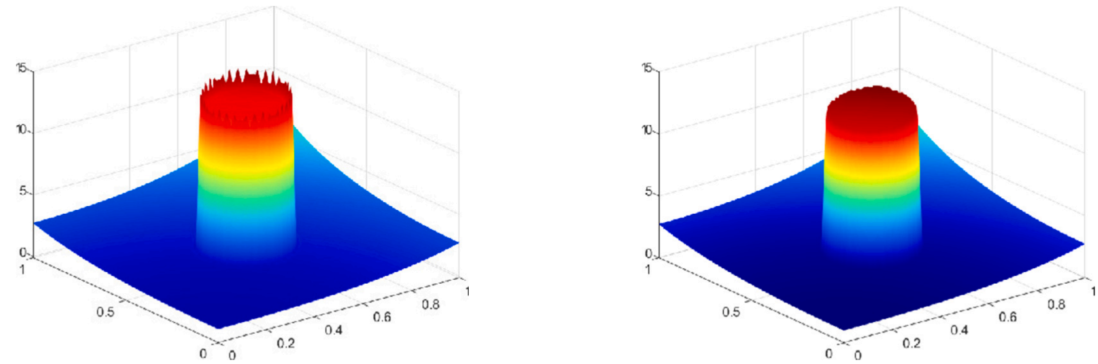

(a) (b)

Fig. 12. The graphs of (a) $Q^4h(x,y)$ and (b) $W^4h(x,y)$ with $m=n=128$.

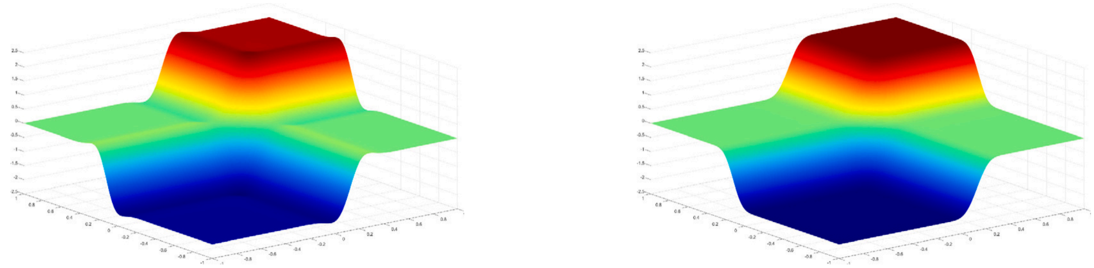

(a) (b)

Fig. 13. The graphs of (a) $Q^1z(x,y)$ and (b) $W^1z(x,y)$ with $m=n=16$.

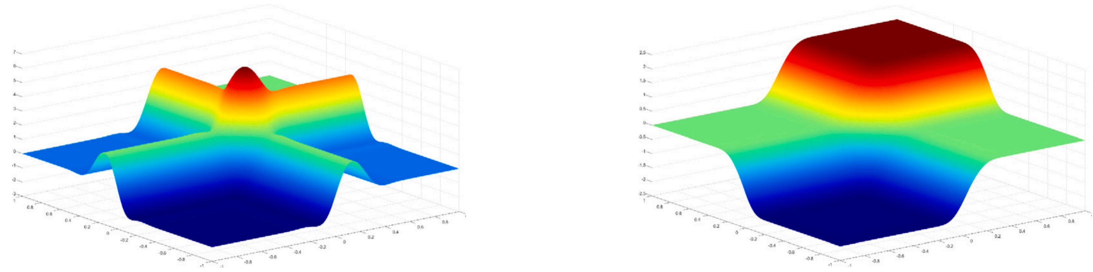

(a) (b)

Fig. 14. The graphs of (a) $Q^2z(x,y)$ and (b) $W^2z(x,y)$ with $m=n=16$.

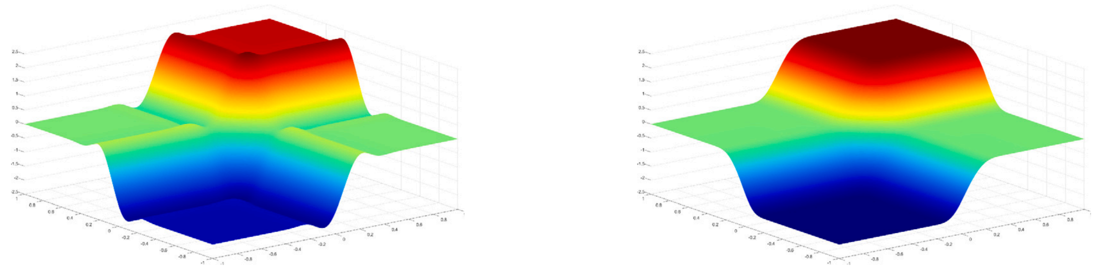

(a) (b)

Fig. 15. The graphs of (a) $Q^3z(x,y)$ and (b) $W^3z(x,y)$ with $m=n=16$.

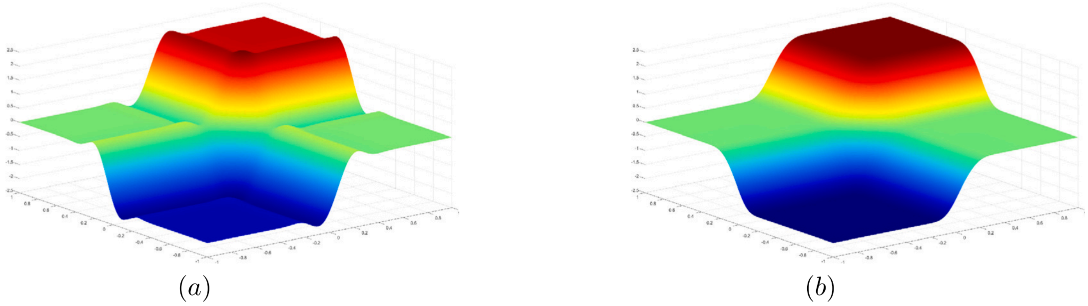

Fig. 16. The graphs of (a) $Q^4 z(x, y)$ and (b) $W^4 z(x, y)$ with $m = n = 16$.

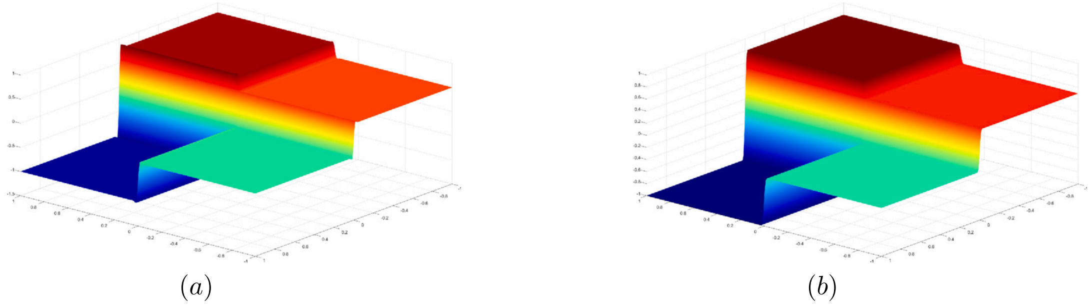

Fig. 17. The graphs of (a) $Q^1 u(x, y)$ and (b) $W^1 u(x, y)$ with $m = n = 128$.

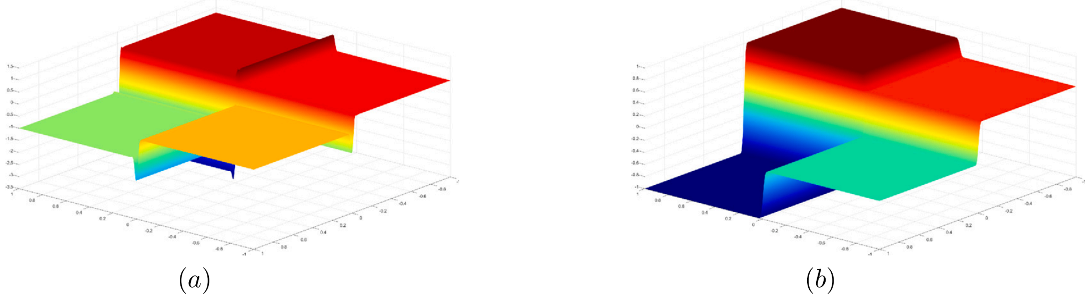

Fig. 18. The graphs of (a) $Q^2 u(x, y)$ and (b) $W^2 u(x, y)$ with $m = n = 128$.

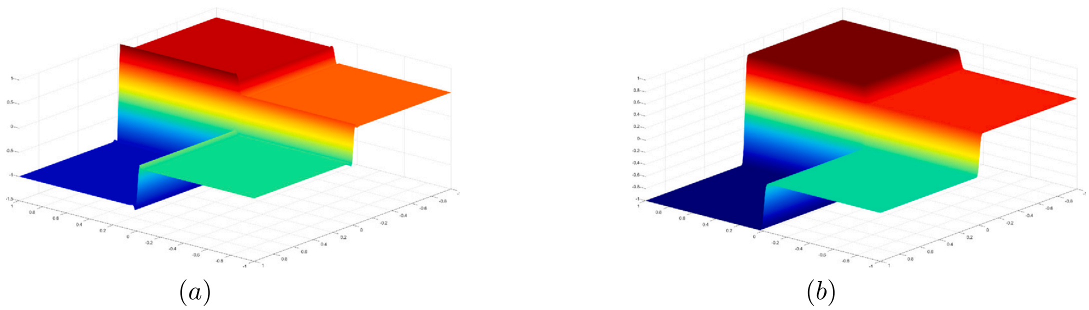

Fig. 19. The graphs of (a) $Q^3 u(x, y)$ and (b) $W^3 u(x, y)$ with $m = n = 128$.

We emphasize that in the example involving the function $z(x, y)$, the function with steep gradient, the oscillations are also eliminated with the nonlinear operators presented in this paper.

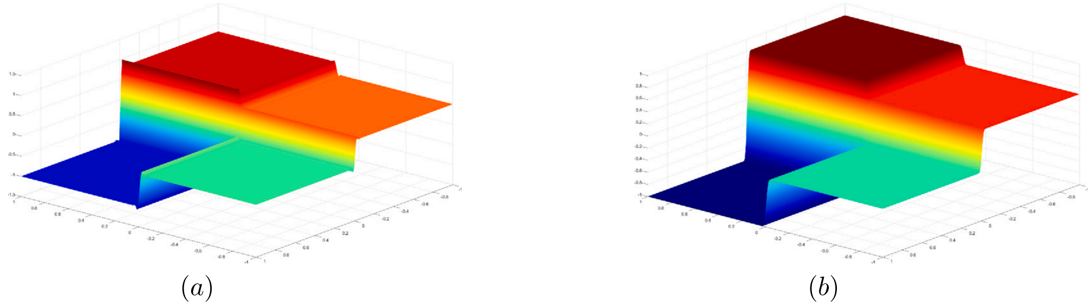

Fig. 20. The graphs of (a) $Q^4u(x,y)$ and (b) $W^4u(x,y)$ with $m=n=128$.

5. Conclusions

In this paper we have considered the space of C^2 quartic splines on uniform criss-cross triangulations and we have proposed a method based on WENO techniques and obtained by modifying classical spline quasi-interpolants in order to approximate piecewise smooth functions avoiding Gibbs phenomenon near discontinuities and, at the same time, maintaining the high-order accuracy in smooth regions, without knowing where the discontinuity is. We have also analysed the convergence properties of the proposed quasi-interpolants and we have provided some numerical and graphical tests confirming the theoretical results.

CRediT authorship contribution statement

Francesc Aràndiga: Writing – review & editing, Writing – original draft, Visualization, Validation, Supervision, Software, Resources, Project administration, Methodology, Investigation, Funding acquisition, Formal analysis, Data curation, Conceptualization. **Sara Remogna:** Writing – review & editing, Writing – original draft, Visualization, Validation, Supervision, Software, Resources, Project administration, Methodology, Investigation, Funding acquisition, Formal analysis, Data curation, Conceptualization.

Acknowledgements

This research has been supported by Spanish MINECO project PID2020-117211GB-I00 and GVA project CIAICO/2021/227. The second author is member of the INdAM Research group GNCS of Italy.

References

[1] E.B. Ameur, D. Barrera, M.J. Ibáñez, D. Sbibih, Near-best operators based on a C^2 quartic spline on the uniform four-directional mesh, Math. Comput. Simul. 77 (2008) 151–160.
[2] F. Aràndiga, A. Baeza, A.M. Belda, P. Mulet, Analysis of WENO schemes for full and global accuracy, SIAM J. Numer. Anal. 49 (2) (2011) 893–915.
[3] F. Aràndiga, A.M. Belda, P. Mulet, Point-value WENO multiresolution applications to stable image compression, J. Sci. Comput. 43 (2) (2010) 158–182.
[4] F. Aràndiga, R. Donat, S. López-Ureña, Nonlinear improvements of quasi-interpolant splines to approximate piecewise smooth functions, Appl. Math. Comput. 448 (2023) 127946.
[5] F. Aràndiga, S. Remogna, Nonlinear 2D C^1 quadratic spline quasi-interpolants on triangulations for the approximation of piecewise smooth functions, Axioms 12 (2023) 1002.
[6] D. Barrera, M.J. Ibáñez, Bernstein-Bézier representation and near-minimally normed discrete quasi-interpolation operators, Appl. Numer. Math. 58 (2008) 59–68.
[7] D. Barrera, M.J. Ibáñez, P. Sablonnière, D. Sbibih, On near-best discrete quasi-interpolation on a four-directional mesh, J. Comput. Appl. Math. 233 (2010) 1470–1477.
[8] R.K. Beatson, M.J.D. Powell, Univariate multiquadric approximation: quasi-interpolation to scattered data, Constr. Approx. 8 (3) (1992) 275–288.
[9] B.D. Bojanov, H.A. Hakopian, A.A. Sahakian, Spline Functions and Multivariate Interpolation, Kluwer Academic Publishers, Dordrecht, 1993.
[10] C. de Boor, K. Höllig, S. Riemenschneider, Box Splines, Springer-Verlag, New York, 1993.
[11] M. Buhmann, J. Jäger, Quasi-Interpolation, Cambridge University Press, 2022.
[12] B. de la Calle Ysern, P. Galán del Sastre, A Lagrange interpolation with preprocessing to nearly eliminate oscillations, Numer. Algorithms (2024), https://doi.org/10.1007/s11075-024-01778-z.
[13] C.K. Chui, Multivariate Splines, CBMS-NSF Regional Conference Series in Applied Mathematics, vol. 54, SIAM, Philadelphia, 1988.
[14] M. Heidari, M. Mohammadi, S. De Marchi, A shape preserving quasi-interpolation operator based on a new transcendental RBF, Dolomites Res. Notes Approx. 14 (2021) 56–73.
[15] M.J. Ibáñez Pérez, Quasi-interpolantes spline discretos de norma casi mínima. Teoría y aplicaciones, PhD Thesis, Universidad de Granada, 2003.
[16] G.S. Jiang, C.W. Shu, Efficient implementation of weighted ENO schemes, J. Comput. Phys. 126 (1) (1996) 202–228.
[17] G.S. Jiang, E. Tadmor, Nonoscillatory central schemes for multidimensional hyperbolic conservation laws, SIAM J. Sci. Comput. 19 (6) (1998) 1892–1917.
[18] M.J.D. Powell, Univariate multiquadric approximation: reproduction of linear polynomials, in: Multivariate Approximation and Interpolation, Springer, 1990, pp. 227–240.
[19] S. Remogna, Constructing good coefficient functionals for bivariate C^1 quadratic spline quasi-interpolants, in: M. Daehlen, et al. (Eds.), Mathematical Methods for Curves and Surfaces, in: LNCS, vol. 5862, Springer-Verlag, Berlin Heidelberg, 2010, pp. 329–346.
[20] S. Remogna, Local spline quasi-interpolants on bounded domains of $\mathbb{R}^2$ and $\mathbb{R}^3$, PhD Thesis, Università degli Studi di Torino - Université de Rennes 1, 2010.
[21] P. Sablonnière, Bases de Bernstein et approximants splines, Thèse de doctorat, Université de Lille, 1982.
[22] P. Sablonnière, On some multivariate quadratic spline quasi-interpolants on bounded domains, in: W. Hausmann, et al. (Eds.), Modern Developments in Multivariate Approximations, in: ISNM, vol. 145, Birkhäuser Verlag, Basel, 2003, pp. 263–278.

[23] P. Sablonnière, Quasi-interpolantes splines sobre particiones uniformes, in: First International Meeting on Approximation Theory of the University of Jaén, June 29-July 2, 2000, Prepublication IRMAR 00-38, Rennes, 2000.

[24] J. Shi, C. Hu, C.W. Shu, A technique of treating negative weights in WENO schemes, J. Comput. Phys. 175 (1) (2002) 108–127.

[25] R.H. Wang, Multivariate Spline Functions and Their Application, Science Press, Kluwer Academic Publishers, Beijing/New York, Dordrecht/Boston/London, 2001.

[26] R.H. Wang, C.J. Li, Bivariate quartic spline spaces and quasi-interpolation operators, J. Comput. Appl. Math. 190 (2006) 325–338.

[27] Z. Wu, R. Schaback, Shape preserving properties and convergence of univariate multiquadric quasi-interpolation, Acta Math. Appl. Sin. 10 (4) (1994) 441–446.